

AIAA 2002-0227

On Constructing Stable Perfectly Matched Layers as an Absorbing Boundary Condition for Euler Equations

Fang Q. Hu
Department of Mathematics and Statistics
Old Dominion University, Norfolk, Virginia 23529

40th AIAA Aerospace Sciences Meeting and Exhibit 14-17 January 2002/Reno, NV

On Constructing Stable Perfectly Matched Layers as an Absorbing Boundary Condition for Euler Equations

Fang Q. Hu*

Department of Mathematics and Statistics

Old Dominion University, Norfolk, Virginia 23529

In a recent work, a stable Perfectly Matched Layer (PML) formulation has been proposed for the linearized Euler equations. The new formulation had been derived under the assumption that the absorption coefficients are constants. In this paper, we present the derivation of the stable PML equations when the absorption coefficients are spatially varying. In addition, PML equations for both the two- and three-dimensional linearized Euler equations will be given. Furthermore, the PML equations are formulated in unsplit physical variables. Numerical examples that demonstrate the validity and effectiveness of the proposed equations are presented.

Introduction

For numerical simulations in an infinite or semiinfinite domain, the physical domain is necessarily truncated and artificial boundaries are formed. Numerical non-reflecting boundary conditions are needed at these artificial boundaries to ensure that out-going disturbances are not reflected. Quite often, nonreflecting boundaries are the sources of the most significant numerical errors in a computation. This is especially true after substantial progresses that have been made in recent years in the discretization methods, such as the utilization of high order schemes and unstructured meshes, as well as the orders-of-magnitude increase in high-performance computing power.

A variety of non-reflecting boundary conditions have been developed in the literature to cope with the open domain problem. The most widely used non-reflecting boundary conditions for the Euler equations are the characteristics based inflow and outflow boundary conditions (eg., [1],[2],[3],[4]). These methods are formed by a generalization of one-dimensional Euler equations to the multi-dimensional cases. The use of characteristics variables is usually straightforward and robust, especially for schemes with upwinding features. The drawback of the characteristics based boundary conditions is that the accuracy can be limited. They usually work the best when the wave is normal to the boundary and their performances can deteriorate when the wave angles deviate from that of a normal incident.

Another type of widely used non-reflecting boundary conditions is based on the far field asymptotic solutions (eg., [5],[6],[7],[8]). The governing equations at the boundary are replaced by suitable forms of

modified partial differential equations based on the asymptotic form of the solution at the far field. This class of methods, when applicable, can be quite accurate. However, because the asymptotic forms are not always available, it may not be applicable in many situations. In addition, to implement the asymptotic-solution-based boundary conditions the computational boundary is necessarily placed at far field to achieve the accuracy. This can result in an increase in computational cost.

A third type of non-reflecting boundary conditions is the buffer zone technique which is actually a group of methods based on various buffer zone techniques. For instances, the computational domain may be extended to create an extra zone where the numerical solution is damped by an application of low-pass filters, grid stretching, numerical damping or a combination of these techniques (eg., [9],[10]); or the mean flow is accelerated to a supersonic velocity toward the end of the added buffer domain thus eliminating the need of a non-reflecting boundary condition (eg., [11],[12]). The accuracy of these methods depends on the gradualness in which the various parameters are varied inside the buffer zone. Moreover, the added buffer zone is usually required to be of substantial length for the method to be effective. The increase in computational cost can be significant.

A recently emerged method of constructing a non-reflecting boundary condition is based on the Perfectly Matched Layer (PML) technique.¹³ In this approach, like the buffer zone method, extra layers of grids are added to the non-reflecting boundaries in which the out-going waves are damped or "absorbed". A major difference between the PML technique and the other buffer zone techniques mentioned earlier is that the equations to be used in the added region are con-

^{*}Associate Professor, Senior Member AIAA

Copyright © 2002 by F. Q. Hu. Published by the American Institute of Aeronautics and Astronautics, Inc. with permission.

structed in such a way that, theoretically, the outgoing waves will not cause any reflection when entering an PML domain, for any frequency and angle of incidence. Because of this, a PML domain is usually very effective as an absorbing boundary condition and requires only a small number of grid points to achieve satisfactory results¹⁴. ¹⁵

The Perfectly Matched Layer technique was first introduced by Berenger¹³ for absorbing electromagnetic waves of the Maxwell equations. For the Euler equations, currently, there are two main PML formulations. The first formulation was given by the author in [14]. Like Berenger's original formulation for the Maxwell equations, it used split variables in the PML domain, i.e., the velocity, pressure and density were split into two independent parts according to the spatial derivative terms in the Euler equations in two space dimensions. The second formulation was given by Abarbanel, Gottlieb and Hesthaven in [16]. This formulation did not split the physical variables but, instead, augmented the Euler equations with additional terms, albeit complicated, so that all waves decay exponentially inside the PML domain. There are also other formulations, notably [17] by Turkel and Yefet, that are aimed at absorbing only the convective acoustic waves when the vorticity and entropy waves are not present.

Unfortunately, both formulations given in [14] and [16] entail exponentially growing solutions that, if not suppressed or eliminated by numerical dissipation or other means, can cause numerical instability in the PML domain and ruin the numerical solution. In [14], the instabilities were suppressed by a use of numerical filtering. In [14], artificial damping terms were added to the PML equations. The instability waves of the PML equations formulated in [14] have been studied at length in [18] by Tam, Auriault and Cambulli. They analyzed the dispersion relations of the linear waves and found that the PML equations of 14 have unstable solutions whenever the mean flow has a component normal to the PML domain interface. They suggested a use of artificial selective damping for the suppression of instability waves since the unstable modes were associated with high wave numbers.

In addition to the instability issue, there is also a well-posedness issue for the formulation given in [14]. The original PML equations constructed by Berenger, 13 for the Maxwell equations, were shown to be only weakly well-posed by Abarbanel and Gottlieb. 19 Later, it was shown by Hesthaven 20 that the formulation given in [14] for the Euler equations was also only weakly well-posed. It was demonstrated that the PML equations proposed in [13] and [14] could become ill-posed by certain low order perturbations. These authors attributed the weakly well-posedness, in part, to the fact that PML equations in [13] and [14] were constructed by splitting the physical vari-

ables. This prompted them to construct PML equations without splitting the physical variables in [16]. However, as mentioned earlier, although the equations given in [16] were shown to be well-posed, they also admitted exponentially growing solutions. A close inspection of the analysis presented in [16] indicates that the unstable modes are associated with low wave numbers. In this case, exponentially growing solutions can be found for k=0 where k is the spatial wave number.

In a recent paper [25], the stability and the well-posedness issues related to the formulation given in [14] were investigated. It was found that, in the presence of a mean flow, there could be acoustic waves that have a positive group velocity but a negative phase velocity in the direction of the mean flow and these waves become actually amplified in the previous formulation, thus, giving rise to the instability. A new stable PML formulation that is perfectly matched to the Euler equations and does not entail exponentially growing solution was presented in [25]. Furthermore, the new formulation was given in unsplit physical variables after treating the PML methodology as a complex change of variables in space (eg., [17],[21],[22],[23],[24]).

The analysis presented in [25] has been carried out under the assumption that the absorption coefficients are constants. In this paper, we show that the analysis presented in [25] can be easily extended to cases where the absorption coefficients are spatially varying. The resulted stable PML equations are, however, the same as those given in [25]. In addition, PML equations for the three-dimensional Euler equations will also be derived in this paper. This will again be formulated in the unsplit physical variables.

The rest of the paper is organized as follows. For completeness, a brief review of the linear waves and their dispersion relations supported by the Euler equations are presented in the next section. We then show that PML formulation with non-constant absorption coefficients can be viewed as a complex change of variables. After reviewing the cause of the instability waves for the split PML version, we derive a stable formulation that is perfectly matched to the Euler equation and does not entail exponentially growing solutions. Both the two- and three-dimensional Euler equations will be considered. Finally, numerical examples are presented to demonstrate the validity and effectiveness of the proposed equations.

Plane waves of the Euler equations

We consider the linearized Euler equations with a uniform mean flow in a vector form,

$$\frac{\partial \mathbf{u}}{\partial t} + \mathbf{A} \frac{\partial \mathbf{u}}{\partial x} + \mathbf{B} \frac{\partial \mathbf{u}}{\partial y} = 0 \tag{1}$$

where

$$\mathbf{u} = \begin{pmatrix} \rho \\ u \\ v \\ p \end{pmatrix}, \ \mathbf{A} = \begin{pmatrix} M & 1 & 0 & 0 \\ 0 & M & 0 & 1 \\ 0 & 0 & M & 0 \\ 0 & 1 & 0 & M \end{pmatrix}, \tag{2}$$

and
$$\mathbf{B} = \begin{pmatrix} 0 & 0 & 1 & 0 \\ 0 & 0 & 0 & 0 \\ 0 & 0 & 0 & 1 \\ 0 & 0 & 1 & 0 \end{pmatrix}$$

Here, ρ is the density, (u,v) is the velocity vector, p is the pressure, and M is the Mach number (i.e., the mean flow non-dimensionalized by the speed of sound). We also assume that the mean flow is subsonic, i.e., M < 1.

It is well known that, when we look for plane waves of the form $\mathbf{u}_0 e^{ik_x x + ik_y y - i\omega t}$, the Euler equations support three types of waves, namely, the acoustic, vorticity and entropy waves. In particular, the dispersion relations of these waves are

$$(\omega - Mk_x)^2 - k_x^2 - k_y^2 = 0 (3)$$

for the acoustic waves and

$$\omega - Mk_x = 0. (4)$$

for the vorticity and entropy waves.

For convenience of discussion, we will use the dispersion relations to express the wave numbers k_x and k_y in terms of the frequency ω and a wave angle ϕ , i.e., we have

$$k_x = \frac{\omega \cos \phi}{1 + M \cos \phi}, \quad k_y = \frac{\omega \sin \phi}{1 + M \cos \phi}$$
 (5)

for the acoustics waves and

$$k_x = \frac{\omega}{M}, \quad k_y = \frac{\omega \tan \phi}{M}$$
 (6)

for the vorticity and entropy waves.²⁶ Then the plane wave solutions of the Euler equations are found to be: acoustic wave,

$$\begin{pmatrix} \rho \\ u \\ v \\ p \end{pmatrix} = A \begin{pmatrix} 1 \\ \cos \phi \\ \sin \phi \\ 1 \end{pmatrix} e^{\frac{i\omega \cos \phi}{1 + M \cos \phi}x + \frac{i\omega \sin \phi}{1 + M \cos \phi}y - i\omega t}, \tag{7}$$

vorticity wave,

$$\begin{pmatrix} \rho \\ u \\ v \\ p \end{pmatrix} = B \begin{pmatrix} 0 \\ -\sin\psi \\ \cos\psi \\ 0 \end{pmatrix} e^{\frac{i\omega}{M}x + \frac{i\omega\tan\psi}{M}y - i\omega t}, \quad (8)$$

and entropy wave,

$$\begin{pmatrix} \rho \\ u \\ v \\ p \end{pmatrix} = C \begin{pmatrix} 1 \\ 0 \\ 0 \\ 0 \end{pmatrix} e^{\frac{i\omega}{M}x + \frac{i\omega \tan x}{M}y - i\omega t}, \qquad (9)$$

where ϕ , ψ and χ are the angles of the wave front normal vectors of the acoustic (A), vorticity (B) and entropy (C) waves, respectively. We note that the wave angles are not assumed to be the same since the three types of waves are kept independent of each other.

PML with variable absorption coefficients

In the PML methodology, absorbing layers are added to the Euler domain so that the waves of all the three kinds mentioned above are absorbed without reflection (Figure 1). A straight forward extension of the PML technique originally proposed by Berenger for the Maxwell equations¹³ suggests a splitting of the Euler equations according to the spatial derivative terms.¹⁴ This results in the following split version of the PML equations for (1),

$$\frac{\partial \mathbf{u}_1}{\partial t} + \sigma_x \mathbf{u}_1 + \mathbf{A} \frac{\partial \mathbf{u}}{\partial x} = 0, \tag{10}$$

$$\frac{\partial \mathbf{u}_2}{\partial t} + \sigma_y \mathbf{u}_2 + \mathbf{B} \frac{\partial \mathbf{u}}{\partial y} = 0, \tag{11}$$

where $\mathbf{u} = \mathbf{u}_1 + \mathbf{u}_2$. σ_x and σ_y are positive absorption coefficients. The conditions on the absorption coefficients are that σ_x be independent of y and σ_y be independent of x with both being assumed zero in the interior Euler domain.

In a recent work [25], an analysis of the split PML equations (10)-(11) has been carried out under the assumption that σ_x and σ_y be constants. It was shown that, for the Euler equation with a mean flow, the split version (10)-(11) can lead to numerical instability inside the PML domain. After an investigation into the cause of instability, a stable reformulation was found and given in [25].

In practical computations, especially when a finite difference scheme is used, σ_x and σ_y are often varied smoothly inside the PML domain. A common spatial variation for the absorption coefficients are of the form

$$\sigma_x = \sigma_x^M \left| \frac{x - x_l}{D_x} \right|^\beta, \tag{12}$$

$$\sigma_y = \sigma_y^M \left| \frac{y - y_l}{D_y} \right|^{\beta}, \tag{13}$$

where x_l or y_l denotes the location of an interface between the Euler and PML domain, and σ_x^M and σ_y^M are the maximum values of σ_x and σ_y respectively.

In addition, D_x and D_y in (12) and (13) denote the thickness of the added PML domains in the x and y directions respectively.

In this paper, we will show that the analysis presented in [25] can be easily extended to cases where σ_x and σ_y are spatially varying. The resulted stable PML equations are, however, the same as those given in [25].

We will begin by re-examining the PML technique as a complex change of variables for space variables x and y when σ_x and σ_y are non-constant. Let us consider the split version (10)-(11) in the frequency domain. By replacing $\frac{\partial}{\partial t}$ with $-i\omega$, we get

$$-i\omega\tilde{\mathbf{u}}_1 + \sigma_x\tilde{\mathbf{u}}_1 + \mathbf{A}\frac{\partial\tilde{\mathbf{u}}}{\partial x} = 0, \tag{14}$$

$$-i\omega\tilde{\mathbf{u}}_2 + \sigma_y\tilde{\mathbf{u}}_2 + \mathbf{B}\frac{\partial\tilde{\mathbf{u}}}{\partial y} = 0, \tag{15}$$

where a tilde indicates the solution in the frequency domain. Dividing equations (14) and (15) by $1+\frac{i\sigma_y}{\omega}$ and $1+\frac{i\sigma_y}{\omega}$, respectively, and subsequently adding the two equations, we can get an equation in the unsplit physical variables,

$$-i\omega\tilde{\mathbf{u}} + \frac{1}{1 + \frac{i\sigma_{x}}{\omega}}\mathbf{A}\frac{\partial\tilde{\mathbf{u}}}{\partial x} + \frac{1}{1 + \frac{i\sigma_{y}}{\omega}}\mathbf{B}\frac{\partial\tilde{\mathbf{u}}}{\partial y} = 0.$$
 (16)

Thus, if we introduce a complex change of variables for x and y as

$$x' = \int_0^x (1 + \frac{i\sigma_x}{\omega}) dx = x + \frac{i}{\omega} \int_0^x \sigma_x dx \tag{17}$$

and

$$y' = \int_0^y (1 + \frac{i\sigma_y}{\omega}) dy = y + \frac{i}{\omega} \int_0^y \sigma_y dy, \tag{18}$$

then

$$\frac{\partial}{\partial x'} = \frac{1}{1 + \frac{i\sigma_x}{\omega}} \frac{\partial}{\partial x}, \quad \frac{\partial}{\partial y'} = \frac{1}{1 + \frac{i\sigma_y}{\omega}} \frac{\partial}{\partial y}$$

and equation (16) becomes

$$-i\omega\tilde{\mathbf{u}} + \mathbf{A}\frac{\partial\tilde{\mathbf{u}}}{\partial x'} + \mathbf{B}\frac{\partial\tilde{\mathbf{u}}}{\partial y'} = 0.$$
 (19)

Here, σ_x and σ_y are assumed to be functions of x and y respectively. The lower limit of the integrals in (17) and (18) can be arbitrarily chosen and has been set to be zero for simplicity. It is easy to see that (19) is exactly the same as the Euler equations when (1) is written in the frequency domain and x and y are replaced by x' and y', respectively. Therefore, the plane wave solutions of (19) should be the same as those in (7)-(9) with x and y being replaced by x' and y'. That

is, the plane waves of (19), and thus the PML equations (10)-(11), when σ_x and σ_y are non-constant, will be

acoustic wave:

$$\begin{pmatrix} \rho \\ u \\ v \\ p \end{pmatrix} = A \begin{pmatrix} 1 \\ \cos \phi \\ \sin \phi \\ 1 \end{pmatrix} e^{\frac{i\omega \cos \phi}{1 + M \cos \phi} x - \frac{\cos \phi}{1 + M \cos \phi} \int_0^x \sigma_x dx}$$
(20)

$$\times e^{\frac{i\omega\sin\phi}{1+M\cos\phi}y - \frac{\sin\phi}{1+M\cos\phi} \int_0^y \sigma_y \, dy - i\omega t}$$

vorticity wave:

$$\begin{pmatrix} \rho \\ u \\ v \\ p \end{pmatrix} = B \begin{pmatrix} 0 \\ -\sin\psi \\ \cos\psi \\ 0 \end{pmatrix} e^{\frac{i\omega}{M}x - \frac{1}{M} \int_0^x \sigma_x dx} \tag{21}$$

$$\times e^{\frac{i\omega \tan \psi}{M}y - \frac{\tan \psi}{M} \int_0^y \sigma_y dy - i\omega t}$$

and entropy wave:

$$\begin{pmatrix} \rho \\ u \\ v \\ p \end{pmatrix} = C \begin{pmatrix} 1 \\ 0 \\ 0 \\ 0 \end{pmatrix} e^{\frac{i\omega \tan \chi}{M}y - \frac{\tan \chi}{M} \int_0^x \sigma_x dx - i\omega t} \quad (22)$$

$$\times e^{\frac{i\omega \tan \psi}{M}y - \frac{\tan \psi}{M} \int_0^y \sigma_y \, dy - i\omega t}$$

We note that the wave eigenvectors in (20)-(22) are the same as those in (7)-(9), while the exponential decaying of the waves has been made possible by the introduction of σ_x and σ_y .

Instability of the split PML equations

A close inspection of the acoustic wave in (20) shows that the solution in (20) can give rise to an instability in the PML domain. Specifically, let us consider the exponential expression involving σ_x in (20),

$$e^{-\frac{\cos\phi}{1+M\cos\phi}\int_0^x \sigma_x dx}. (23)$$

Since σ_x is always positive, the expression in (23) will be exponentially decaying only if the wave is

where ϕ is the angle of the wave front normal vector as defined in (5). Here, the direction of wave propagation

is determined by the group velocity \mathbf{v}_g , in that a wave is right-going or left-going if the x-component of the group velocity is positive or negative, respectively. In the presence of a mean flow, however, as we will see below, the group velocity is not always in the same direction as that of the phase velocity and there now exist right-going waves with $\cos \phi < 0$.

For the acoustic waves in the Euler equations, the group velocity, by dispersion relation (3), is

$$\mathbf{v}_g = (\frac{\partial \omega}{\partial k_x}, \frac{\partial \omega}{\partial k_y}) = (M + \cos \phi, \sin \phi)$$
 (24)

where ϕ is as defined in (5) (see, eg., [27],[28]). Obviously, there could be right-going waves where $M+\cos\phi>0$ but $\cos\phi<0$, as illustrated in Figure 3. For these waves, therefore, the wave amplitude will actually be exponentially growing after entering the PML domain, giving rise to the instability. The unstable wavenumbers are shown in Figure 4.

On the other hand, for the horizontal y-layers where $\sigma_x = 0$ no instability will occur, since the y-component of the group velocity is in the same direction as that of the phase velocity. In addition, the vorticity and entropy waves do not concern us because they travel with the mean flow in the x-direction and will be exponentially decaying according to (21) and (22).

Stable PML equations in unsplit physical variables

As we have seen in the previous section, the instability of the split equations (10)-(11) is caused by the existence of convective acoustic waves that have a positive group velocity but a negative phase velocity in the x-direction. Therefore, to construct stable PML equations, we first use a transformation so that in the transformed coordinates the acoustic waves of the Euler equations become non-convective and the group velocities of all linear waves are in the same direction as that of the phase velocities. We then apply the PML technique to the transformed equations. This technique has been successfully applied in [25] for constant σ_x and σ_y . As we will see, it will work for variable absorption coefficients as well. Furthermore, although the original PML was implemented in split variables, the splitting is actually not necessary and the new PML formulation will be given in unsplit physical variable.

Following similar transformations used in several previous works in dealing with the convective wave equation (see, eg., [5],[16],[17] and [29]), we introduce new variables \bar{x}, \bar{y} and \bar{t} as follows,

$$\bar{x} = x, \ \bar{y} = \sqrt{1 - M^2}y, \ \bar{t} = t + \frac{M}{1 - M^2}x.$$
 (25)

The corresponding transformed wavenumbers and frequency are

$$\bar{k}_x = k_x + \frac{M}{1 - M^2} \omega, \ \bar{k}_y = \frac{1}{\sqrt{1 - M^2}} k_y, \ \bar{\omega} = \omega.$$
 (26)

In the transformed variables, the Euler equation (1) is found to be

$$\left(\mathbf{I} + \frac{M}{1 - M^2}\mathbf{A}\right)\frac{\partial \mathbf{u}}{\partial \bar{t}} + \mathbf{A}\frac{\partial \mathbf{u}}{\partial \bar{x}} + \sqrt{1 - M^2}\mathbf{B}\frac{\partial \mathbf{u}}{\partial \bar{y}} = 0$$
(27)

where I is the identity matrix. It is also easy to find that the dispersion relations for (27) in the transformed wavenumbers and frequency are

$$\frac{\bar{\omega}^2}{(1-M^2)^2} - \bar{k}_x^2 - \bar{k}_y^2 = 0$$

for the acoustic waves and

$$\frac{\bar{\omega}}{1 - M^2} - M\bar{k}_x = 0.$$

for the vorticity and entropy waves. As we can see, the acoustic waves are now non-convective in the transformed variables and, further, the direction of propagation for the vorticity and entropy waves is unaltered.

Now, we apply the PML complex change of variables (18) to the transformed equation (27). In the frequency domain, we modify (27) to be

$$-i\bar{\omega}\left(\mathbf{I} + \frac{M}{1 - M^2}\mathbf{A}\right)\tilde{\mathbf{u}} + \frac{1}{1 + \frac{i\sigma_x}{2}}\mathbf{A}\frac{\partial\tilde{\mathbf{u}}}{\partial\bar{x}}$$
(28)

$$+\sqrt{1-M^2}\frac{1}{1+\frac{i\sigma_y}{\bar{\Omega}}}\mathbf{B}\frac{\partial \tilde{\mathbf{u}}}{\partial \bar{y}}=0.$$

After multiplying (28) by $(1 + \frac{i\sigma_x}{\bar{\omega}})(1 + \frac{i\sigma_y}{\bar{\omega}})$, we get

$$\left(\mathbf{I} + \frac{M}{1 - M^2}\mathbf{A}\right) \left[-i\bar{\omega}\tilde{\mathbf{u}} + (\sigma_x + \sigma_y)\tilde{\mathbf{u}} + \frac{i}{\bar{\omega}}\sigma_x\sigma_y\tilde{\mathbf{u}} \right]$$

$$+\left(1+\frac{i\sigma_y}{\bar{\omega}}\right)\mathbf{A}\frac{\partial\tilde{\mathbf{u}}}{\partial\bar{x}}+\left(1+\frac{i\sigma_y}{\bar{\omega}}\right)\sqrt{1-M^2}\mathbf{B}\frac{\partial\tilde{\mathbf{u}}}{\partial\bar{u}}=0, (29)$$

The above can be written back in the time domain by introducing an auxiliary variable **q** such that

$$\frac{\partial \mathbf{q}}{\partial \bar{t}} = \mathbf{u} \text{ and } \tilde{\mathbf{q}} = \frac{i}{\bar{\omega}} \tilde{\mathbf{u}}.$$

Then, equation (29) in the time domain is

$$\left(\mathbf{I} + \frac{M}{1 - M^2}\mathbf{A}\right) \left[\frac{\partial \mathbf{u}}{\partial \bar{t}} + (\sigma_x + \sigma_y)\mathbf{u} + \sigma_x \sigma_y \mathbf{q}\right] + \mathbf{A}\frac{\partial \mathbf{u}}{\partial \bar{x}} + \sigma_y \mathbf{A}\frac{\partial \mathbf{q}}{\partial \bar{x}}$$

$$+\sqrt{1-M^2}\mathbf{B}\frac{\partial\mathbf{u}}{\partial\bar{u}}+\sigma_x\sqrt{1-M^2}\mathbf{B}\frac{\partial\mathbf{q}}{\partial\bar{u}}=0.$$

Finally, when expressed in the original variables x, y and t, we get the following new formulation of the PML equations,

$$\frac{\partial \mathbf{u}}{\partial t} + \mathbf{A} \frac{\partial \mathbf{u}}{\partial x} + \mathbf{B} \frac{\partial \mathbf{u}}{\partial y} + \sigma_y \mathbf{A} \frac{\partial \mathbf{q}}{\partial x} + \sigma_x \mathbf{B} \frac{\partial \mathbf{q}}{\partial y}$$

$$+(\sigma_x + \sigma_y)\mathbf{u} + \sigma_x\sigma_y\mathbf{q} + \frac{\sigma_x M}{1 - M^2}\mathbf{A}(\mathbf{u} + \sigma_y\mathbf{q}) = 0, (30)$$

$$\frac{\partial \mathbf{q}}{\partial t} = \mathbf{u}.\tag{31}$$

These two equations, (30)-(31), are the same as those given in [25] and do not entail exponentially growing solutions. For well-posedness issues^{30,31} of the proposed equations, we refer to the analysis given in [25].

It is also straight forward to find that the plane wave solutions to (30)-(31) are

acoustic wave:

$$\begin{pmatrix} \rho \\ u \\ v \\ p \end{pmatrix} = A \begin{pmatrix} 1 \\ \cos \phi \\ \sin \phi \\ 1 \end{pmatrix} e^{\frac{i\omega \cos \phi}{1 + M \cos \phi}x - \frac{(M + \cos \phi)}{(1 - M^2)(1 + M \cos \phi)} \int_0^x \sigma_x dx}$$
(32)

$$imes e^{rac{i\omega\sin\phi}{1+M\cos\phi}y-rac{\sin\phi}{1+M\cos\phi}\int_0^y\,\sigma_y\,dy-i\omega t}$$

vorticity wave:

$$\begin{pmatrix} \rho \\ u \\ v \\ p \end{pmatrix} = B \begin{pmatrix} 0 \\ -\sin\psi \\ \cos\psi \\ 0 \end{pmatrix} e^{\frac{i\omega}{M}x - \frac{1}{(1-M^2)M}} \int_0^x \sigma_x dx$$

$$\times e^{\frac{i\omega\tan\psi}{M}y - \frac{\tan\psi}{M}} \int_0^y \sigma_y dy - i\omega t$$
(33)

and entropy wave:

$$\begin{pmatrix} \rho \\ u \\ v \\ p \end{pmatrix} = C \begin{pmatrix} 1 \\ 0 \\ 0 \\ 0 \end{pmatrix} e^{\frac{i\omega}{M}x - \frac{1}{(1-M^2)M} \int_0^x \sigma_x dx}$$
(34)

$$\times e^{\frac{i\omega\tan\psi}{M}y - \frac{\tan\psi}{M}\int_0^y \sigma_y dy - i\omega t}$$

where ϕ , ψ and χ are, again, the angles of the wave front normal vectors. From (32)-(34), we can show easily that the solutions are perfectly matched at any vertical interface where σ_y is the same on both sides of the interface and at any horizontal interface where σ_x is the same on both sides.¹⁴ This includes the interfaces between the Euler domain and a PML domain as well as the interfaces between two PML domains

such as those at the corner layers. When compared with (20), the acoustic wave in (32) is now absorbed correctly according to the group velocity. In addition, the absorption rate in the x-direction is increased by a factor of $1/(1-M^2)$. This means that the absorption rate in the x-direction will be larger than that in the y-direction if the values of absorption coefficients are the same.

It is important to note that the auxiliary variable ${\bf q}$ is only needed inside the PML domains, because the spatial derivative $\frac{\partial {\bf q}}{\partial x}$ is only required when $\sigma_y \neq 0$ which only happens inside a horizontal y-layer or a corner layer and $\frac{\partial {\bf q}}{\partial y}$ is only required when $\sigma_x \neq 0$ inside a vertical x-layer or corner layer. This situation is illustrated in Figure 1. As a result, we do not need to know ${\bf q}$ in the Euler domain. Therefore, ${\bf q}$ is neither computed nor stored inside the Euler domain.

Simplified PML equations

We note that at a vertical x-layer or horizontal y-layer, one of the absorption coefficients is zero and, accordingly, a simpler form of (30) results. Specifically, we have these simplified equations:

at a vertical x-layer $(\sigma_y = 0)$, we solve

$$\frac{\partial \mathbf{u}}{\partial t} + \mathbf{A} \frac{\partial \mathbf{u}}{\partial x} + \mathbf{B} \frac{\partial \mathbf{u}}{\partial y} + \sigma_x \mathbf{B} \frac{\partial \mathbf{q}}{\partial y} + \sigma_x \mathbf{u} + \frac{\sigma_x M}{1 - M^2} \mathbf{A} \mathbf{u} = 0;$$
(35)

at a horizontal y-layer ($\sigma_x = 0$), we solve

$$\frac{\partial \mathbf{u}}{\partial t} + \mathbf{A} \frac{\partial \mathbf{u}}{\partial x} + \mathbf{B} \frac{\partial \mathbf{u}}{\partial y} + \sigma_y \mathbf{A} \frac{\partial \mathbf{q}}{\partial x} + \sigma_y \mathbf{u} = 0.$$
 (36)

In both cases, the equation for \mathbf{q} is (31). At a corner layer, of course, the full version of (30)-(31) should be used. This situation is depicted in Figure 4.

Three-dimensional PML equations

In this section, we show that the technique used in deriving the two-dimensional PML equations (30)-(31) can be easily extended to three-dimensional problems. Let the three-dimensional linearized Euler Equations be written in the matrix form

$$\frac{\partial \mathbf{u}}{\partial t} + \mathbf{A} \frac{\partial \mathbf{u}}{\partial x} + \mathbf{B} \frac{\partial \mathbf{u}}{\partial y} + \mathbf{C} \frac{\partial \mathbf{u}}{\partial z} = 0 \tag{37}$$

where

$$\mathbf{u} = \begin{bmatrix} \rho \\ u \\ v \\ w \\ p \end{bmatrix}, \mathbf{A} = \begin{bmatrix} M & 1 & 0 & 0 & 0 \\ 0 & M & 0 & 0 & 1 \\ 0 & 0 & M & 0 & 0 \\ 0 & 0 & 0 & M & 0 \\ 0 & 1 & 0 & 0 & M \end{bmatrix}$$

After applying the following transformation to (37),

$$\bar{x} = x, \ \bar{y} = \sqrt{1 - M^2}y, \ \bar{z} = \sqrt{1 - M^2}z, \ \bar{t} = t + \frac{M}{1 - M^2}x$$

we get

$$\left(\mathbf{I} + \frac{M}{1-M^2}\mathbf{A}\right)\frac{\partial \mathbf{u}}{\partial \bar{t}} + \mathbf{A}\frac{\partial \mathbf{u}}{\partial \bar{x}} + \sqrt{1-M^2}\mathbf{B}\frac{\partial \mathbf{u}}{\partial \bar{y}} + \sqrt{1-M^2}\mathbf{C}\frac{\partial \mathbf{u}}{\partial \bar{z}} = 0$$

To apply the PML technique, we modify the above equation in the frequency domain as

$$-i\bar{\omega}\left(\mathbf{I} + \frac{M}{1 - M^2}\mathbf{A}\right)\mathbf{u} + \frac{1}{1 + \frac{i\sigma_x}{\bar{\omega}}}\mathbf{A}\frac{\partial\mathbf{u}}{\partial\bar{x}}$$
$$+ \frac{\sqrt{1 - M^2}}{1 + \frac{i\sigma_y}{\bar{\omega}}}\mathbf{B}\frac{\partial\mathbf{u}}{\partial\bar{y}} + \frac{\sqrt{1 - M^2}}{1 + \frac{i\sigma_z}{\bar{\omega}}}\mathbf{C}\frac{\partial\mathbf{u}}{\partial\bar{z}} = 0$$
(38)

Multiplying (38) by $(1 + \frac{i\sigma_x}{\overline{\omega}})(1 + \frac{i\sigma_y}{\overline{\omega}})(1 + \frac{i\sigma_z}{\overline{\omega}})$, we get

$$\left(\mathbf{I} + \frac{M}{1 - M^2}\mathbf{A}\right) \left[-i\bar{\omega}\mathbf{u} + (\sigma_x + \sigma_y + \sigma_z)\mathbf{u} \right]$$
$$+ \frac{i}{\bar{\omega}}(\sigma_x\sigma_y + \sigma_x\sigma_z + \sigma_y\sigma_z)\mathbf{u} - \frac{1}{\bar{\omega}^2}\sigma_x\sigma_y\sigma_z\mathbf{u}$$

$$+(1+\frac{i\sigma_y}{\bar{\omega}})(1+\frac{i\sigma_z}{\bar{\omega}})\mathbf{A}\frac{\partial\mathbf{u}}{\partial\bar{x}}+(1+\frac{i\sigma_x}{\bar{\omega}})(1+\frac{i\sigma_z}{\bar{\omega}})\sqrt{1-M^2}\mathbf{B}\frac{\partial\mathbf{u}}{\partial\bar{y}}$$

$$+\left(1+\frac{i\sigma_x}{\bar{\omega}}\right)\left(1+\frac{i\sigma_y}{\bar{\omega}}\right)\sqrt{1-M^2}\mathbf{C}\frac{\partial\mathbf{u}}{\partial\bar{z}}=0$$
 (39)

This can be rewritten in the time domain by introducing auxiliary variables \mathbf{q}_1 and \mathbf{q}_2 as shown below. Thus, the PML equations for the three-dimensional Euler equations are the following,

$$\frac{\partial \mathbf{u}}{\partial t} + \mathbf{A} \frac{\partial \mathbf{u}}{\partial x} + \mathbf{B} \frac{\partial \mathbf{u}}{\partial y} + \mathbf{C} \frac{\partial \mathbf{u}}{\partial z}
+ (\sigma_y + \sigma_z) \mathbf{A} \frac{\partial \mathbf{q}_1}{\partial x} + (\sigma_x + \sigma_z) \mathbf{B} \frac{\partial \mathbf{q}_1}{\partial y} + (\sigma_x + \sigma_y) \mathbf{C} \frac{\partial \mathbf{q}_1}{\partial z}
+ \sigma_y \sigma_z \mathbf{A} \frac{\partial \mathbf{q}_2}{\partial x} + \sigma_x \sigma_z \mathbf{B} \frac{\partial \mathbf{q}_2}{\partial y} + \sigma_x \sigma_y \mathbf{C} \frac{\partial \mathbf{q}_2}{\partial z}
+ (\sigma_x + \sigma_y + \sigma_z) \mathbf{u} + (\sigma_x \sigma_y + \sigma_x \sigma_z + \sigma_y \sigma_z) \mathbf{q}_1 + \sigma_x \sigma_y \sigma_z \mathbf{q}_2
+ \frac{\sigma_x M}{1 - M^2} \mathbf{A} [\mathbf{u} + (\sigma_y + \sigma_z) \mathbf{q}_1 + \sigma_y \sigma_z \mathbf{q}_2] = 0 \quad (40)$$

$$\frac{\partial \mathbf{q}_1}{\partial t} = \mathbf{u} \tag{41}$$

$$\frac{\partial \mathbf{q}_2}{\partial t} = \mathbf{q}_1 \tag{42}$$

The absorption coefficients σ_x , σ_y and σ_z can be constants or functions of x, y and z respectively, as illustrated in Figure 5. Again, it is easy to verify that the auxiliary variables \mathbf{q}_1 and \mathbf{q}_2 are only required inside the added PML domain and need not to be known inside the Euler domain. Equation (40) can be further simplified whenever any of the absorption coefficients is zero. In particular, \mathbf{q}_2 is not needed in any region where two of the absorption coefficients are zero.

Numerical Examples

To demonstrate the validity and effectiveness of the PML equations, three numerical examples will be presented. In all the examples, both the Euler equations and the PML equations are solved numerically by a finite difference scheme. Specifically, the spatial derivatives are discretized by a 4th-order 7-point central difference scheme given in [8] (the DRP scheme), combined with a 5-point boundary closure scheme given in [32]. The time integration is carried out by a 4thorder Runge-Kutta scheme that has been optimized for minimal dissipation and dispersion errors³³ (the LD-DRK56 scheme). Further details of the scheme can be found in [33] and [34]. Only two-dimensional examples will be shown in this paper. As mentioned earlier, the auxiliary variable q is only introduced in the PML domains and is neither computed nor stored in the interior Euler domain. To verify stability, no numerical filtering or damping is used in all the computations reported here.

Since a wide stencil is used in the finite difference scheme, the absorption coefficients are varied gradually inside a PML domain. The variations of absorption coefficients used in the computations are

$$\sigma_x = \sigma_m (1 - M^2) \left| \frac{x - x_l}{D} \right|^{\beta}, \ \ \sigma_y = \sigma_m \left| \frac{y - y_l}{D} \right|^{\beta},$$
 (43)

where x_l or y_l denotes the location where the PML domain starts, and D is the width of the PML domain. A factor of $1-M^2$ has been included in σ_x so that the absorption rates remain the same in both the x and y directions. Values of $\sigma_m \Delta x = 2$, where Δx is the grid size, and $\beta = 2$ are used for all the computations.

At the end of the PML domain, no special boundary condition is needed except those that are necessary to maintain the numerical stability of the scheme. According to the characteristics of (30)-(31), for a subsonic mean flow, we should specify three boundary conditions at the left side of the computational domain and one boundary condition each at the other three sides. For the results reported here, we apply these simple boundary conditions at end points of the PML domains,

at
$$x = X_{max}, y = Y_{min}$$
 and $y = Y_{max}$: $p = 0$,

at inflow
$$x = X_{min} : p = \rho = v = \theta$$
,

in which $[X_{min}, X_{max}] \times [Y_{min}, Y_{max}]$ denotes the entire computational domain as indicated in Figure 1. Other forms of characteristics based boundary conditions are equally applicable. Alternatively, it is also possible to apply periodic boundary conditions since the numerical solution decays exponentially toward all the boundaries.

Acoustic pulse inside a duct

In this example, we simulate the propagation of an acoustic pulse inside a duct in the presence of a mean flow of Mach number M=0.8. The computational domain is $[-110,110] \times [-50,50]$ where solid walls are located at $y=\pm 50$. A uniform grid of $\Delta x=\Delta y=1$ has been used. Two PML domains of thickness $10\Delta x$ are included at either end of the open duct. The acoustic pulse is initiated at t=0 by the initial condition:

$$\rho = u = v = 0, p = e^{-(\ln 2)\frac{(x+50)^2+y^2}{6^2}}.$$

Figure 6 shows the pressure contours inside the duct at t=20,60,110,150 and 200. As the acoustic pulse is convected downstream, it is reflected by the duct walls. However, no visible reflection from the open boundary is detected. This shows that the PML can be an effective non-reflecting boundary for duct acoustics without assuming any specific modal form of the acoustics waves.

Acoustic source

In the second example, we solve the Euler equations with the following source term added to the equation for the pressure:

$$P(x, y, t) = \sin(\Omega t)e^{-(\ln 2)\frac{(x+20)^2 + y^2}{9}}.$$

The frequency of the source is $\Omega=0.03\pi$ and the mean flow Mach number is M=0.8. Due to the mean flow, the acoustic wave has a larger wavelength at downstream boundary than that at the upstream boundary. The Euler domain is $[-100,100] \times [-100,100]$. The source is located at (x,y)=(-20,0). Figure 7 shows the pressure contours of the numerical solution at t=600. The PML domains for this calculation have a width $D=10\Delta x$. The calculated pressure as a function of time at two chosen locations, (x,y)=(100,10) and (-100,10), is plotted in Figure 8. Also plotted are the reference solution computed using a larger domain. Excellent agreement is found. This example shows that PML equations can be effective for absorbing long waves as well as short waves.

Vorticity source

In the third example, we simulate the convection of vorticity waves generated by a vortex source. To simulate the vortex generator, the following vorticity source terms are added to the Euler equations (1),

$$U(x, y, t) = -\sin(\Omega t) y e^{-(\ln 2)\frac{(x+50)^2 + y^2}{9}}$$
(44)

$$V(x,y,t) = \sin(\Omega t)(x+50)e^{-(\ln 2)\frac{(x+50)^2+y^2}{9}} \qquad (45)$$

where U(x, y, t) and V(x, y, t) are added to the right hand sides of u and v momentum equations respectively. Figure 9 shows the v velocity contours of the generated vorticity waves and their exit through the computational domain. While the vortices are absorbed inside the PML domain, no visible reflection is detected. Thus, the proposed PML equations offer an attractive way to construct an effective absorbing boundary condition for the linearized Euler equations.

Conclusions

A stable Perfectly Matched Layer formulation has been derived for the linearized Euler equations in two and three space dimensions. The derivation has been carried out under the assumption that the absorption coefficients may be spatially varying. The new formulation is also given in unsplit physical variables, which should facilitate its implementation in many practical schemes. Numerical examples indicate that the proposed PML equations can be used as an effective absorbing boundary condition.

References

¹K.W. Thompson, "Time-dependent boundary conditions for hyperbolic systems II", *Journal of Computational Physics*, Vol. 89, 439-461, 1990.

²M. B. Giles, "Non-reflecting boundary conditions for Euler equation calculations", *AIAA Journal*, Vol. 28, 2050-2058, 1990.

³T. J. Poinsot and S. K. Lele, "Boundary conditions for direct simulations of compressible viscous flows", *Journal of Computational Physics*, Vol. 101, 104-129, 1992.

⁴R. L. Higdon, "Numerical absorbing boundary conditions for the wave equation", *Math Computation*, Vol. 49, 65-90, 1987.

⁵A. Bayliss and Eli Turkel, "Radiation boundary conditions for wave-like equations", *Communications on Pure and Applied Mathematics*, Vol. 33, 708-725, 1980.

⁶B. Enquist and A. Majda, "Absorbing boundary conditions for the numerical simulation of waves", *Math. Computation*, Vol. 31, 629-651, 1977.

⁷T. Hagstrom and S. I. Hariharan, "Accurate boundary conditions for exterior problems in gas dynamics", *Math. Computation*, Vol. 51, 581-597, 1988.

⁸C. K. W. Tam and J. C. Webb, "Dispersion-Relation-Preserving schemes for computational acoustics", *Journal of Computational Physics*, Vol. 107, 262-281, 1993.

⁹M. Israeli and S. Orszag, "Approximation of Radiation Boundary Conditions", *Journal of computational Physics*, Vol. 41, 115-135, 1981.

 $^{10}{\rm T.}$ Colonious, S. K. Lele and P. Moin, "Boundary conditions for direct computation of aerodynamic sound generation", AIAA Journal, Vol. 31, 1574-1582, 1993.

¹¹C. L. Streett and M. G. Macaraeg, "Spectral multi-domain for large-scale fluid dynamics simulations", *Int. Journal Appl. Numer. Math.*, Vol. 6, 123-139, 1989.

 12 S. Ta'asan and D. M. Nark, "An absorbing buffer zone technique for acoustic wave propagation", AIAA paper 95-0164, 1995.

¹³ J-P Berenger, "A perfectly matched layer for the absorption of electromagnetic waves", *Journal of computational Physics*, Vol. 114, 185-200, 1994.

¹⁴F. Q. Hu, "On absorbing boundary conditions of linearized Euler equations by a perfectly matched layer", *Journal of Com*putational Physics, Vol. 129, 201-219, 1996.

¹⁵F. Q. Hu, "On Perfectly Matched Layer as an absorbing boundary condition", AIAA paper 96-1664, 1996.

¹⁶S. Abarbanel, D. Gottlieb and J. S. Hesthaven, "Well-posed perfectly matched layers for advective acoustics", *Journal of Computational Physics*, Vol. 154, 266-283, 1999.

- ¹⁷E. Turkel and A. Yefet, "Absorbing PML boundary layers for wave-like equations", *Applied Numerical Mathematics*, Vol. 27, 533-557, 1998.
- ¹⁸C. K. W. Tam, L. Auriault and F. Cambulli, "Perfectly Matched Layer as an absorbing boundary condition for the linearized Euler equations in open and ducted domains", *Journal* of Computational Physics, Vol. 144, 213-234, 1998.
- $^{19}\mathrm{S.}$ Abarbanel and D. Gottlieb, "A mathematical analysis of the PML method", Journal of Computational Physics, Vol. 134, 357-363, 1997.
- ²⁰ J. S. Hesthaven, "On the analysis and construction of perfectly matched layers for the linearized Euler equations", *Journal of Computational Physics*, Vol. 142, 129-147, 1998.
- $^{21}{\rm F.}$ Collino and P. Monk, "The perfectly matched layer in curvilinear coordinates", SIAM~J.~Sci,~Comp, Vol. 19, No. 6, P. 2016, 1998.
- ²²S. D. Gedney, "An anisotropic perfectly matched layerabsorbing medium for the truncation of FDTD lattices", *IEEE Trans. Antennas Propagation*, Vol. 44, P. 1630, 1996.
- ²³L. Zhao and A. C. Cangellaris, "GT-PML: generalized theory of perfectly match layers and its application to the reflectionless truncation of finite-difference time-domain grids", *IEEE Trans. Microwave Theory Tech.*, Vol. 44., 2555-2563, 1996.
- ²⁴R. W. Ziolkowski, "Time-derivative Lorentz material model-based absorbing boundary condition", *IEEE Trans. Antennas Propagation*, Vol. 45, P. 1530, 1997.
- ²⁵F. Q. Hu, "A stable, Perfectly Matched Layer for linearized Euler equations in unsplit physical variables", *Journal of Computational Physics*, In press, 2001.
- $^{26}\,\mathrm{P.}$ M. Morse and K. U. Ingard, Theoretical Acoustics, McGraw-Hill, 1968.
- $^{27}\mathrm{J.}$ Lighthill, Waves~In~Fluids, P. 311 and P. 327, Cambridge, 1978.
- ²⁸G. B. Whitham, *Linear and Nonlinear Waves*, John Wiley & Sons, 1974.
- ²⁹S. I. Hariharan, J. R. Scott and K. L. Kreider, "A potential-theoretic method for far-field sound radiation calculations", Journal of Computational Physics, Vol. 164, 143-164, 2000.
- ³⁰ J. C. Strikwerda, Finite Difference Schemes and Partial Differential Equations, Wadsworth & Broke/Cole, 1989.
- ³¹ B. Gustafsson, H. O. Kreiss and J. Oliger, *Time dependent problems and difference methods*, John Wiley & Sons, 1995.
- $^{32}\mathrm{J.}$ Gary, Journal of Computational Physics, Vol. 26, P. 339, 1978.
- ³³F. Q. Hu, M. Y. Hussaini and J. L. Manthey, "Low-dissipation and low dispersion Runge-Kutta schemes for computational acoustics", *Journal of Computational Physics*, Vol. 124, 177-191, 1996.
- ³⁴F. Q. Hu and J. L. Manthey, "Application of PML absorbing boundary conditions to the Benchmark problems of Computational Aeroacoustics", Second Computational Aeroacoustics (CAA) Workshop on Benchmark Problems, eds Tam and Hardin, NASA CP 3352, 119-151, 1997.

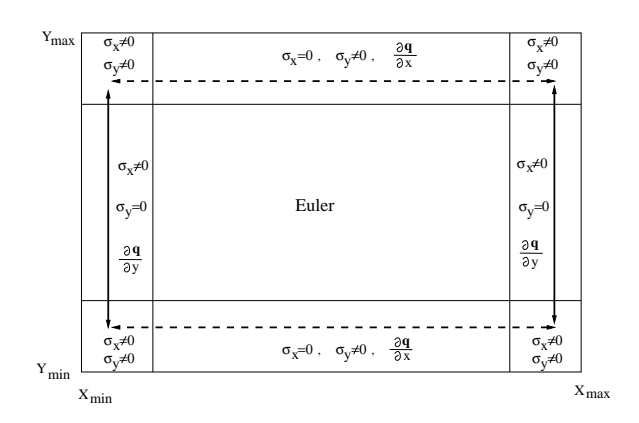


Figure 1. Illustration of a computational domain combining the Euler and PML domains. Solid arrowed lines indicate the domains where $\partial \mathbf{q}/\partial y$ is needed and dashed arrowed lines indicate the domains where $\partial \mathbf{q}/\partial x$ is needed.

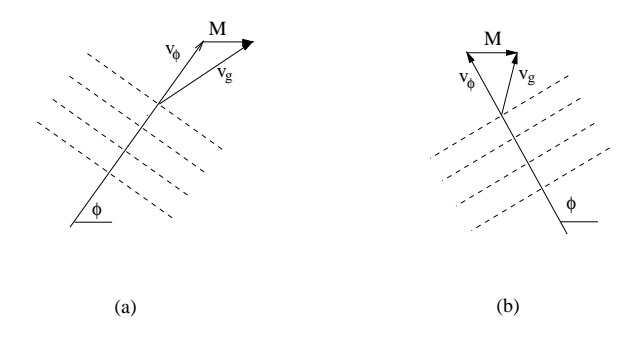


Figure 2. A schematic drawing showing the relation between the wave front normal vector $\mathbf{v}_{\phi} = (\cos \phi, \sin \phi)$ and the group velocity \mathbf{v}_g of the acoustic wave in the presence of a mean flow of Mach number M. (a) A right-going wave with $\cos \phi > 0$; (b) a right-going wave with $\cos \phi < 0$

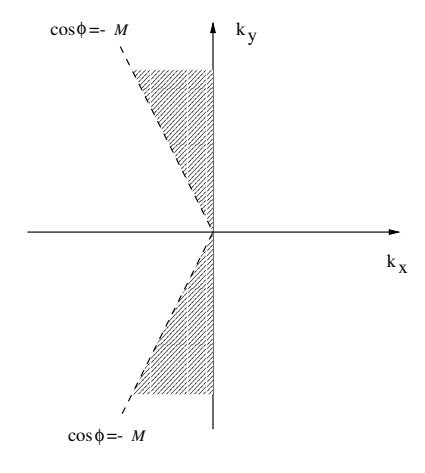


Figure 3. Shaded are the wavenumbers of the acoustic waves that will be amplified when they enter the PML domain.

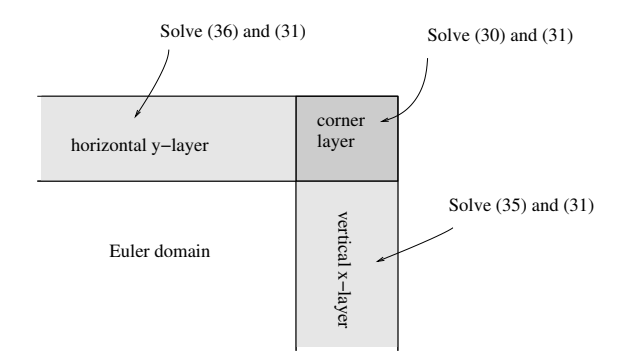


Figure 4. An illustration of simplified PML equations for different layers.

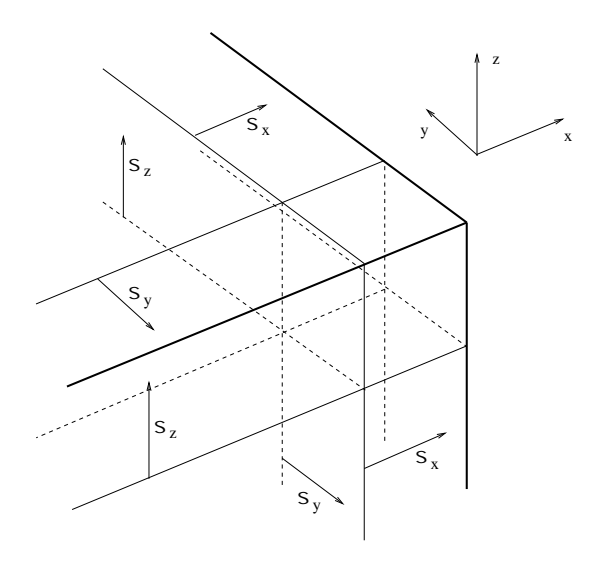
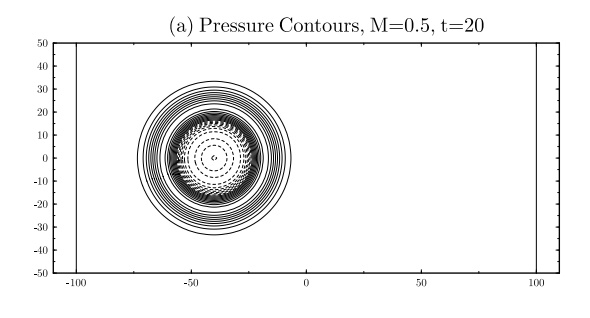
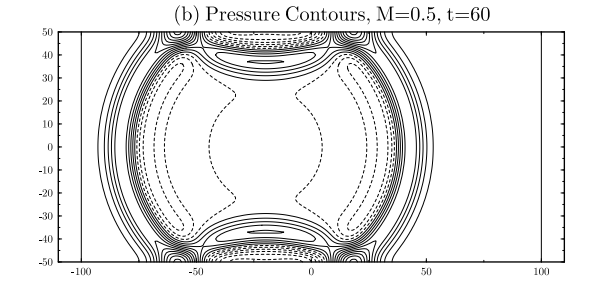
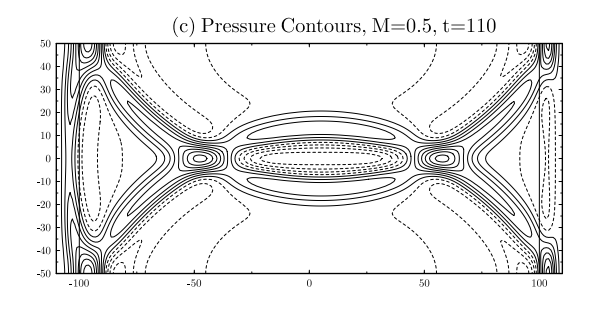
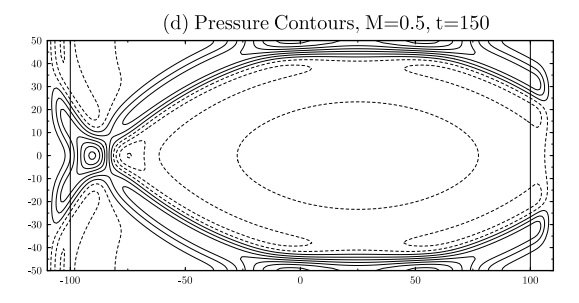


Figure 5. A schematic of PML configuration in three space dimensions. The arrows indicate the direction of increase in the value of the absorption coefficients.









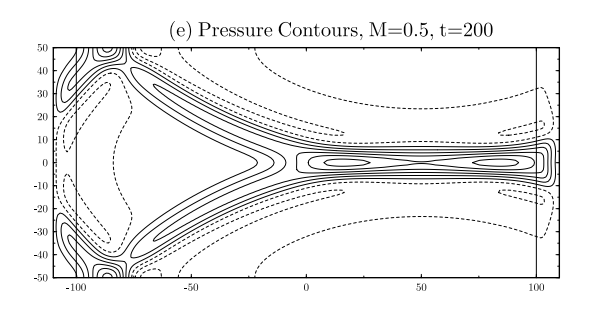


Figure 6 (a)-(e). Propagation of an acoustic pulse inside a duct with solid walls. M = 0.8, $D = 10\Delta x$.

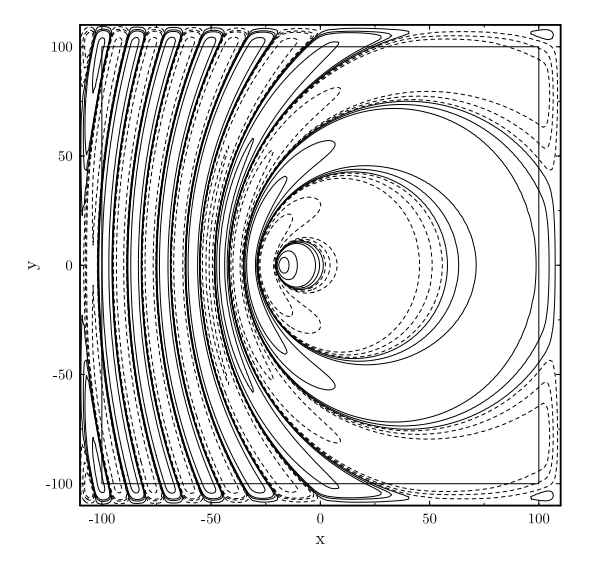


Figure 7. Contours of the pressure p at levels ± 0.1 , ± 0.05 , ± 0.01 , ± 0.005 and ± 0.001 . M=0.8, $D=10\Delta x$. t=600.

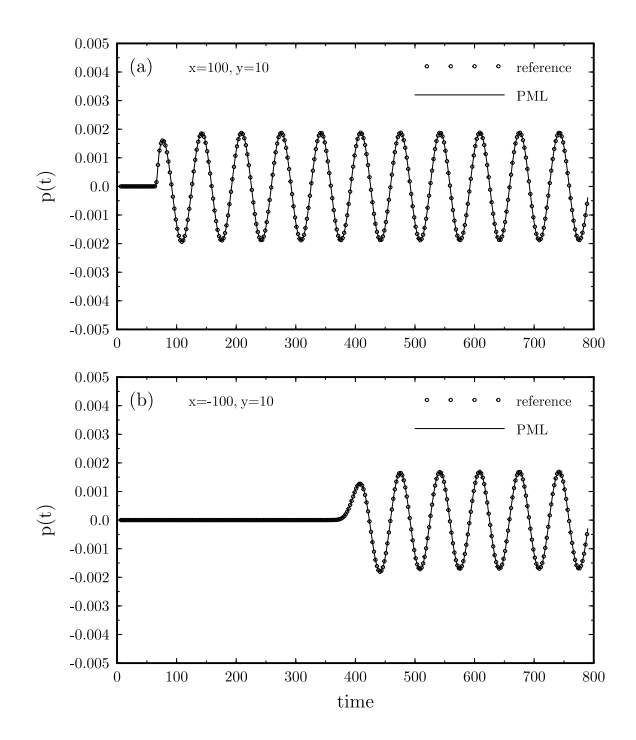
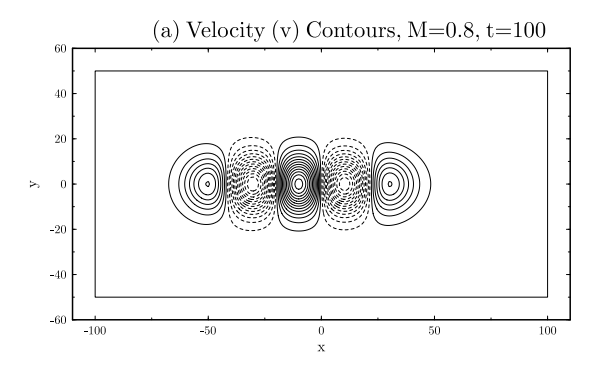
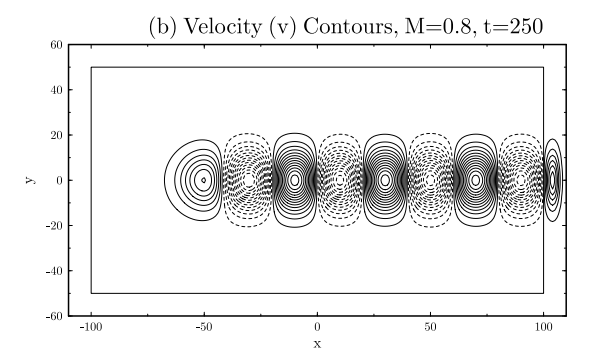


Figure 8. Pressure as a function of time at two selected points. (a) (x,y)=(100,10) and (b) (x,y)=(-100,10). M=0.8. $D=10\Delta x$; —— PML solution; circles, reference solution.





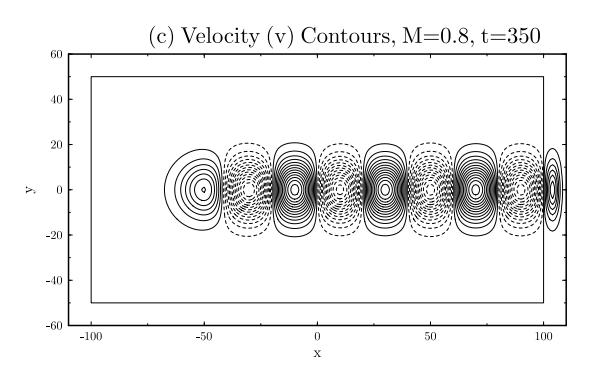


Figure 9 (a)-(c). Propagation of vorticity waves generated by source terms given in (44) and (45). $M=0.8,\,D=10\Delta x.$